Biomedical Optics EXPRESS

Analytical optimization of the ablation efficiency at normal and non-normal incidence for generic super Gaussian beam profiles

Samuel Arba-Mosquera, PhD[*] and Shwetabh Verma, MSc

SCHWIND eye-tech-solutions, Kleinostheim, D-63801, Germany
[*] *samuel.arba.mosquera@eye-tech.net*

Abstract: We suggest a general method to determine the optimum laser parameters for maximizing the ablation efficiency for different materials (in particular human cornea) at different incidence angles. The model is comprehensive and incorporates laser beam characteristics and ablative spot properties. The model further provides a method to convert energy fluctuations during ablation to equivalent ablation deviations in the cornea. The proposed model can be used for calibration, verification and validation purposes of laser systems used for ablation processes at relatively low cost and would directly improve the quality of results.

©2013 Optical Society of America

OCIS codes: (170.1020) Ablation of tissue; (330.7335) Visual optics, refractive surgery; (140.3295) Laser beam characterization; (140.3425) Laser stabilization.

References and links

1. I. G. Pallikaris and D. S. Siganos, "Excimer laser in situ keratomileusis and photorefractive keratectomy for correction of high myopia," J. Refract. Corneal Surg. **10**(5), 498–510 (1994).
2. K. Ditzen, H. Huschka, and S. Pieger, "Laser in situ keratomileusis for hyperopia," J. Cataract Refract. Surg. **24**(1), 42–47 (1998).
3. M. A. el Danasoury, G. O. Waring 3rd, A. el Maghraby, and K. Mehrez, "Excimer laser in situ keratomileusis to correct compound myopic astigmatism," J. Refract. Surg. **13**(6), 511–520 (1997).
4. S. Arba-Mosquera and M. Shraiki, "Analysis of the PMMA and cornea temperature rise during excimer laser ablation," J. Mod. Opt. **57**(5), 400–407 (2010).
5. S. Arba-Mosquera and N. Triefenbach, "Analysis of the cornea-to-PMMA ablation efficiency rate," J. Mod. Opt. **59**(10), 930–941 (2012).
6. C. B. O'Donnell, J. Kemner, and F. E. O'Donnell, Jr., "Ablation smoothness as a function of excimer laser delivery system," J. Cataract Refract. Surg. **22**(6), 682–685 (1996).
7. B. Müller, T. Boeck, and C. Hartmann, "Effect of excimer laser beam delivery and beam shaping on corneal sphericity in photorefractive keratectomy," J. Cataract Refract. Surg. **30**(2), 464–470 (2004).
8. M. Mrochen, M. Kaemmerer, P. Mierdel, and T. Seiler, "Increased higher-order optical aberrations after laser refractive surgery: A problem of subclinical decentration," J. Cataract Refract. Surg. **27**(3), 362–369 (2001).
9. M. Mrochen, R. R. Krueger, M. Bueeler, and T. Seiler, "Aberration-sensing and wavefront-guided laser in situ keratomileusis: Management of decentered ablation," J. Refract. Surg. **18**(4), 418–429 (2002).
10. N. M. Taylor, R. H. Eikelboom, P. P. van Sarloos, and P. G. Reid, "Determining the accuracy of an eye tracking system for laser refractive surgery," J. Refract. Surg. **16**(5), S643–S646 (2000).
11. M. Bueeler, M. Mrochen, and T. Seiler, "Effect of spot size, ablation depth, and eye-tracker latency on the optical outcome of corneal laser surgery with a scanning spot laser," In Ophthalmic Technologies XIII SPIE, **4951**, 150-160 (2003).
12. D. Zadok, C. Carrillo, F. Missiroli, S. Litwak, N. Robledo, and A. S. Chayet, "The effect of corneal flap on optical aberrations," Am. J. Ophthalmol. **138**(2), 190–193 (2004).
13. M. Mrochen and T. Seiler, "Influence of corneal curvature on calculation of ablation patterns used in photorefractive laser surgery," J. Refract. Surg. **17**(5), S584–S587 (2001).
14. P. S. Hersh, K. Fry, and J. W. Blaker, "Spherical aberration after laser in situ keratomileusis and photorefractive keratectomy. Clinical results and theoretical models of etiology," J. Cataract Refract. Surg. **29**(11), 2096–2104 (2003).
15. J. R. Jimenez, R. G. Anera, L. J. Barco, and E. Hita, "Effect on laser-ablation algorithms of reflection losses and nonnormal incidence on the anterior cornea," Appl. Phys. Lett. **81**(8), 1521–1523 (2002).

#192124 - $15.00 USD Received 11 Jun 2013; revised 11 Jul 2013; accepted 11 Jul 2013; published 24 Jul 2013
(C) 2013 OSA

16. R. G. Anera, J. R. Jiménez, L. Jiménez del Barco, and E. Hita, "Changes in corneal asphericity after laser refractive surgery, including reflection losses and non-normal incidence upon the anterior cornea," Opt. Lett. **28**(6), 417–419 (2003).
17. D. Cano, S. Barbero, and S. Marcos, "Comparison of real and computer-simulated outcomes of LASIK refractive surgery," J. Opt. Soc. Am. A **21**(6), 926–936 (2004).
18. J. R. Jiménez, F. Rodríguez-Marín, R. G. Anera, and L. Jiménez Del Barco, "Deviations of Lambert-Beer's law affect corneal refractive parameters after refractive surgery," Opt. Express **14**(12), 5411–5417 (2006).
19. C. Dorronsoro, D. Cano, J. Merayo-Lloves, and S. Marcos, "Experiments on PMMA models to predict the impact of corneal refractive surgery on corneal shape," Opt. Express **14**(13), 6142–6156 (2006).
20. C. Roberts, "Biomechanics of the cornea and wavefront-guided laser refractive surgery," J. Refract. Surg. **18**(5), S589–S592 (2002).
21. D. Huang, M. Tang, and R. Shekhar, "Mathematical model of corneal surface smoothing after laser refractive surgery," Am. J. Ophthalmol. **135**(3), 267–278 (2003).
22. C. Roberts, "Biomechanical customization: The next generation of laser refractive surgery," J. Cataract Refract. Surg. **31**(1), 2–5 (2005).
23. C. R. Munnerlyn, S. J. Koons, and J. Marshall, "Photorefractive keratectomy: a technique for laser refractive surgery," J. Cataract Refract. Surg. **14**(1), 46–52 (1988).
24. G. Yoon, S. Macrae, D. R. Williams, and I. G. Cox, "Causes of spherical aberration induced by laser refractive surgery," J. Cataract Refract. Surg. **31**(1), 127–135 (2005).
25. A. Vogel and V. Venugopalan, "Mechanisms of pulsed laser ablation of biological tissues," Chem. Rev. **103**(2), 577–644 (2003).
26. S. Arba-Mosquera and D. de Ortueta, "Geometrical analysis of the loss of ablation efficiency at non-normal incidence," Opt. Express **16**(6), 3877–3895 (2008).
27. G. H. Pettit and M. N. Ediger, "Corneal-tissue absorption coefficients for 193- and 213-nm ultraviolet radiation," Appl. Opt. **35**(19), 3386–3391 (1996).
28. D. N. Nikogosyan and H. Gorner, "Laser-induced photodecomposition of amino acids and peptides: extrapolation to Corneal Collagen," IEEE J. Sel. Top. Quantum Electron. **5**(4), 1107–1115 (1999).
29. B. T. Fisher and D. W. Hahn, "Development and numerical solution of a mechanistic model for corneal tissue ablation with the 193 nm argon fluoride excimer laser," J. Opt. Soc. Am. A **24**(2), 265–277 (2007).
30. H. J. Huebscher, U. Genth, and T. Seiler, "Determination of excimer laser ablation rate of the human cornea using in vivo Scheimpflug videography," Invest. Ophthalmol. Vis. Sci. **37**(1), 42–46 (1996).
31. M. Mrochen, V. Semshichen, R. H. Funk, and T. Seiler, "Limitations of erbium:YAG laser photorefractive keratectomy," J. Refract. Surg. **16**(1), 51–59 (2000).
32. G. H. Pettit, "The ideal excimer beam for refractive surgery," J. Refract. Surg. **22**(9), S969–S972 (2006).
33. B. Neuenschwander, "High throughput structuring: basics, limitations and needs," Bern University of Applied Sciences, Engineering and Information Technology, Laser Surface Engineering.
34. D. Huang and M. Arif, "Spot size and quality of scanning laser correction of higher order wavefront aberrations," J. Refract. Surg. **17**(5), S588–S591 (2001).
35. A. Guirao, D. R. Williams, and S. M. MacRae, "Effect of beam size on the expected benefit of customized laser refractive surgery," J. Refract. Surg. **19**(1), 15–23 (2003).
36. G. H. Pettit, "The Alcon/Summit/Autonomous perspective on fixed vs. variable spot ablation," J. Refract. Surg. **17**(5), S592–S593 (2001).
37. J. E. A. Pedder, A. S. Holmes, and P. E. Dyer, "Improved model for the angular dependence of excimer laser ablation rates in polymer materials," Appl. Phys. Lett. **95**(17), 174105 (2009).
38. J. R. Jiménez, J. J. Castro, C. Ortiz, and R. G. Anera, "Testing a model for excimer laser-ablation rates on corneal shape after refractive surgery," Opt. Lett. **35**(11), 1789–1791 (2010).
39. C. Dorronsoro, S. Schumacher, P. Pérez-Merino, J. Siegel, M. Mrochen, and S. Marcos, "Effect of air-flow on the evaluation of refractive surgery ablation patterns," Opt. Express **19**(5), 4653–4666 (2011).

Introduction

The available methods allow for the correction of refractive defects such as myopia [1], hyperopia [2], or astigmatism [3]. Achieving accurate clinical outcomes and reducing the likelihood of a retreatment procedure are major goals of refractive surgery. For that, accurately calibrated lasers with high stability are required. For the surgeons, it is difficult to adequately compensate the deviations in ablation from the planned ablation in their nomograms in order to achieve the desired refractive correction. Despite its empirical nature, some nomogram factors enabled surgeons to plan their treatments with a reasonable degree of success.

Recently, we have published [4,5], a general method to analyze the ablation rate for different materials (in particular in the human cornea and poly-methyl-methacrylate (PMMA)) and its associated findings. The understanding of the underlying processes may in

#192124 - $15.00 USD Received 11 Jun 2013; revised 11 Jul 2013; accepted 11 Jul 2013; published 24 Jul 2013
(C) 2013 OSA

both cases help improving systems. It is well known that a successful surgery depends on the correct design of an ablation profile, precise delivery of laser energy to the corneal position, and reliable understanding of the corneal tissue response. A large number of factors influence the laser ablation and outcome. Among them, laser energy delivery technique [6,7], ablation decentration and registration [8,9], eye tracking [10, 11], flap [12], physical characteristics of ablation [13–19], wound-healing and biomechanics of the cornea [20–24], have been explored to predict or explain the clinically observed discrepancy between intended and actual outcomes. The quantification of influence of these factors is important for providing the optimal outcome for the refractive surgeries.

The main purpose of this paper is to determine the optimum laser parameters for maximizing the ablation efficiency. With a flying-spot laser, the resulting ablation profile must be deconvolved into a series of shot positions, often requiring more than 10,000 shots for the surgery.

With the introduction of the laser technologies for refractive surgery, the change of the corneal curvature to compensate in a controlled manner for refractive errors of the eye [23], is more accurate than ever. The procedure is nowadays a successful technique, due to its sub-micrometric precision and the high predictability and repeatability of corneal ablation accompanied by minimal side effects. The topic "Optimization of the ablation efficiency" is still worth to be analyzed and considered, because its clinical implications are not yet deeply explored. The real impact of ablation resolution in laser corneal refractive surgery is still discussed in a controversial way. The aim of this work is to provide a simple and understandable theoretical frame explaining a possible method of ablation resolution optimization.

Materials and methods

The interaction of 193 nm excimer laser radiation and corneal tissue is a complex process, involving both ultraviolet photochemistry and rapid thermal decomposition [25]. With the flying-spot laser system, the corneal ablation behavior is mainly governed by the relationship between the per-pulse tissue ablation depth and the fluence (energy per illuminated area) of the incident laser radiation.

At the laser-cornea-interaction, the laser beam incidents and splits into a propagated/absorbed beam inside the cornea and a reflected beam.

Corneal remodeling is essentially similar to any other form of micro-machining. The lasers used in micro-machining are normally pulsed excimer lasers, where the time length of the pulses is very short compared to the time period between the pulses. Although the pulses contain little energy, given the small size of the beams, energy density can be high for this reason; and given the short pulse duration, the peak power provided can be high.

Many parameters have to be considered in designing an efficient laser ablation. One is the selection of the appropriate wavelength (193.3 ± 0.8 nm for ArF) with optimum depth of absorption in tissue, which results in a high-energy deposition in a small volume for a speedy and complete ablation. The second parameter is a short pulse duration to maximize peak power and minimize thermal conductivity to the adjacent tissue (ArF excimer based $\tau<20$ ns).

The radiant exposure is a measure of the density of energy that governs the amount of corneal tissue removed by a single pulse. In excimer laser refractive surgery, this energy density must exceed 40-50 mJ/cm^2. The depth of a single impact relates to the fluence, and also the thermal load per pulse increases with increasing fluence. Knowing the fluence and details of the energy profile of the beam (size, profile, and symmetry), we can estimate the depth, diameter and volume of the ablation impact.

The ablated volume of a single spot is much smaller than the total ablation volume. Due to this, multiple laser pulses are sequentially delivered on to the cornea. Each laser pulse locally ablates a small amount of corneal tissue. The global process is an integral effect of the local process of each individual laser pulse. A higher spot profile gives a higher ablation volume

#192124 - $15.00 USD Received 11 Jun 2013; revised 11 Jul 2013; accepted 11 Jul 2013; published 24 Jul 2013
(C) 2013 OSA

but a lower resolution. On the other hand, a lower spot profile increases the resolution at the cost of increasing the ablation time and the thermal effects due to increased number of laser pulses invested in ablating the same volume. Additionally, using laser pulses with a very low spot profile close to the threshold of the material would mean only imparting thermal effects instead of making any real ablation. All these factors make the energy selection a sensitive criterion. While selecting the optimum energy, a delicate balance needs to be accounted for, between the material thresholds, resolution of the laser pulses, thermal effects of the material and the total ablation time required.

Several metrics interesting for optimization of the ablation rate can be defined:

Calculation of the ablation depth per laser pulse

The depth of ablation impact for non-normal incidence can be calculated as [26],

$$d_S = \frac{1}{\alpha}\ln\left(\frac{I_0 \cdot \cos\theta}{I_{Th}}\right) \tag{1}$$

where d_S is the depth of a single spot, I_0 is the peak radiant exposure (at the axis of the laser beam), I_{Th} is the ablation threshold for radiant exposure for the irradiated tissue or material below which no ablation occurs, θ is the angle of incidence, and α the absorption coefficient of the irradiated tissue or material.

Calculation of the spot diameter

The spot diameter of ablation impact for non-normal incidence can be calculated as [26],

$$FP = \frac{2 \cdot R_0}{\cos\theta}\left[\frac{\ln\left(\frac{I_0 \cdot \cos\theta}{I_{Th}}\right)}{2}\right]^{\frac{1}{2 \cdot N}} \tag{2}$$

where R_0 is the beam size when the radiant exposure falls to $1/e^2$ its peak value, N is the super-gaussian order of the beam profile (where N = 1 represents a simple Gaussian beam profile, and N = ∞ represents a flat-top beam profile), and FP (foot-print) is the diameter of a single spot.

Calculation of the spot area

The spot area of ablation impact for non-normal incidence can be calculated as:

$$A_S = \frac{\pi \cdot R_0^2}{\cos\theta}\left[\frac{\ln\left(\frac{I_0}{I_{Th}}\right) \cdot \ln\left(\frac{I_0 \cdot \cos\theta}{I_{Th}}\right)}{4}\right]^{\frac{1}{2 \cdot N}} \tag{3}$$

where A_S is the ablated area of a single spot.

Calculation of the ablation volume per laser pulse

The volume of ablation impact for non-normal incidence can be calculated as [26],

#192124 - $15.00 USD Received 11 Jun 2013; revised 11 Jul 2013; accepted 11 Jul 2013; published 24 Jul 2013
(C) 2013 OSA

$$V_S = \frac{\pi \cdot R_0^{\,2}}{\alpha \cdot 2^{\frac{1}{N}}} \left[\ln\left(\frac{I_0}{I_{Th}} \right) \right]^{\frac{1}{N}} \left[\frac{N}{N+1} \ln\left(\frac{I_0}{I_{Th}} \right) + \ln(\cos\theta) \right] \tag{4}$$

where V_S is the volume of a single spot.

For human corneal tissue irradiated with nanosecond pulses at 193nm, the ablation threshold takes values of about 40-50 mJ/cm^2 [27,28], and the absorption coefficient is about 3.33-3.99 μm^{-1} [27,28], although Fisher and Hahn [29], described a global ablation model that incorporates a dynamically changing tissue absorption coefficient and that substantially deviates from a static Beer-Lambert model. We chose values of 46.5 mJ/cm^2 for the ablation threshold, 0.5 mm radius for beam size and 3.485 μm^{-1} as absorption coefficient of the human corneal tissue. We chose a value of 2 for the super-gaussian order of the beam profile, unless otherwise stated. These are the typical values for 193nm excimer laser. For other wavelengths in use (namely 206nm and 213nm), the presented results would not vary much as the ablation threshold for these wavelengths is very similar to the value we use.

Relationship between pulse energy and radiant exposure

For a super-Gaussian profile, the following equation applies for the radiant exposure [5],

$$I_0 = \frac{2^{\frac{1}{N}} \cdot N \cdot E_{Pulse}}{\pi \cdot R_0^2 \cdot \Gamma\left(\frac{1}{N} \right)} \tag{5}$$

where E_{Pulse} is total energy of the laser pulse and Γ is the gamma function (the general factorial function for non-integer arguments, $\Gamma(x) = \int_0^\infty t^{z-1} \cdot e^{-t} \cdot dt$).

Metrics for ablation efficiency

Metrics for ablation efficiency can be in general defined as:

$$Metric_{AblationEfficiency} = \frac{ValuableMetric}{E_{Pulse}} \tag{6}$$

where the metric is the value considered for optimization and the valuable metric one of the measures previously defined.

Optimization involves minimizing the pulse energy incident on a single spot in order to minimize the thermal effects on the tissue as well as the effects on the neighboring laser spots, while maintaining the delicate balance between thermal effects and the resolution of the treatment. The pulse energy is directly related to the peak radiant exposure.

Optimization process

Since I_0 is linear with E_{Pulse} (As per Eq. (5)), we can optimize this metric for I_0:

$$\frac{\partial Metric_{AblationEfficiency}}{\partial I_0} = 0 \tag{7}$$

The value of I_0 calculated from this expression is the optimum fluence for the considered metric.

#192124 - $15.00 USD Received 11 Jun 2013; revised 11 Jul 2013; accepted 11 Jul 2013; published 24 Jul 2013
(C) 2013 OSA

Determination of the fluctuations in corneal ablation from the fluctuations observed in the laser energy output

Since I_0 is linear with E_{Pulse}, the deviations in corneal ablation from the fluctuations observed in the laser energy output (ΔEnergy) can be equated as:

$$\Delta ValuableMetric = \Delta Energy \frac{\partial ValuableMetric}{\partial I_0} \tag{8}$$

Results

Optimum ablation depth per laser pulse

The optimum spot depth at non-normal incidence can be calculated from Eq. (1):

$$I_{0,Optimum} = \frac{I_{Th}}{\cos\theta} e \tag{9}$$

$$d_S = \frac{1}{\alpha} \tag{10}$$

Here the term $I_{0,Optimum}$ represents the optimum fluence. The optimum fluence for spot depth computes 126 mJ/cm^2.

Optimum spot diameter

The optimum spot diameter at non-normal incidence can be calculated from Eq. (2):

$$I_{0,Optimum} = \frac{I_{Th}}{\cos\theta} e^{\frac{1}{2\cdot N}} \tag{11}$$

$$FP = \frac{2\cdot R_0}{\cos\theta}\left(\frac{1}{4\cdot N}\right)^{\frac{1}{2\cdot N}} \tag{12}$$

The optimum fluence for spot size depends also on the supergaussian order, and for normal incidence computes 77 mJ/cm^2 for simple gaussian profiles and I_{Th} for flat-top profiles. Considering N = 2 as normal beam profiles ("slightly saturated Gaussian", a typical shape for excimer lasers), the optimum fluence for spot size computes to be 60 mJ/cm^2.

Optimum spot area

The optimum spot area at non-normal incidence can be calculated from Eq. (3):

$$I_{0,Optimum} = \frac{I_{Th}}{\cos\theta} e^{\frac{1}{N}} \tag{13}$$

$$A_S = \frac{\pi\cdot R_0^2}{\cos\theta}\left(\frac{1}{2\cdot N}\right)^{\frac{1}{N}} \tag{14}$$

The optimum fluence for spot area depends also on the supergaussian order, and for normal incidence computes 126 mJ/cm^2 for simple gaussian profiles and I_{Th} for flat-top profiles. Considering N = 2 as normal beam profiles, the optimum fluence for spot area computes 77 mJ/cm^2.

Optimum ablation volume per laser pulse

The optimum spot volume at non-normal incidence can be calculated from Eq. (4):

#192124 - $15.00 USD Received 11 Jun 2013; revised 11 Jul 2013; accepted 11 Jul 2013; published 24 Jul 2013
(C) 2013 OSA

$$I_{0,Optimum} = \frac{I_{Th}}{\cos\theta} e^{\frac{N+1}{N}} \tag{15}$$

$$V_S = \frac{\pi \cdot R_0^{\,2}}{2^{\frac{1}{N}} \cdot \alpha} \left[\frac{N+1}{N} - \ln(\cos\theta) \right]^{\frac{1}{N}} \left\{ 1 + \ln\left[(\cos\theta)^{\frac{1}{N+1}} \right] \right\} \tag{16}$$

The optimum fluence for spot volume depends also on the supergaussian order, and for normal incidence computes 344 mJ/cm^2 for simple gaussian profiles and 126 mJ/cm^2 for flat-top profiles. Considering N = 2 as normal beam profiles, the optimum fluence for spot volume computes 208 mJ/cm^2.

Table 1. Calculated Optimized Values for Different Metrics using Typical Specifications and Normal Incidence

Metric	Spot Depth	Spot Diameter	Spot Area	Spot Volume
Optimum fluence	126 mJ/cm^2	60 mJ/cm^2	77 mJ/cm^2	208 mJ/cm^2
Value for Metric	287 nm	595 µm	0.393 mm^2	195 pl
Value for Metric/ Optimum fluence	2.27013 nm/(mJ/cm^2)	9.9586 µm/(mJ/cm^2)	0.00512 mm^2/(mJ/cm^2)	0.93653 pl/(mJ/cm^2)
Pulse Energy	0.622 mJ	0.294 mJ	0.377 mJ	1.026 mJ

The optimized values are calculated for the following typical specifications:
R_0, the beam radius when the radiant exposure falls to $1/e^2$ its peak value = 0.5 mm
N, super-Gaussian order of the beam profile = 2
I_{Th}, the ablation threshold for radiant exposure for the irradiated tissue (Human Cornea) = 46.5 mJ/cm^2
α, the absorption coefficient of the irradiated tissue (Human Cornea) = 3.485 µm^{-1}

Table 1 represents the optimized value for each metric (value to achieve optimum fluence), obtained using the above equations and under the typical condition described in the methods for normal beam profiles. In table and figures, the value of the super-gaussian order of the beam profile, N = 2 if not stated otherwise.

Figures 1(a) and 1(b) represents the behavior of each metric with respect to a series of randomly chosen values of radiant exposures. The optimum for each metric corresponds to the values in Table 1. Figures 2(a) and 2(b) represents the optimum fluence for each metric at non-normal incidence. In Fig. 2(b) the 4 mm radial distance represents a typical value of ablation zone (8 mm diameter).

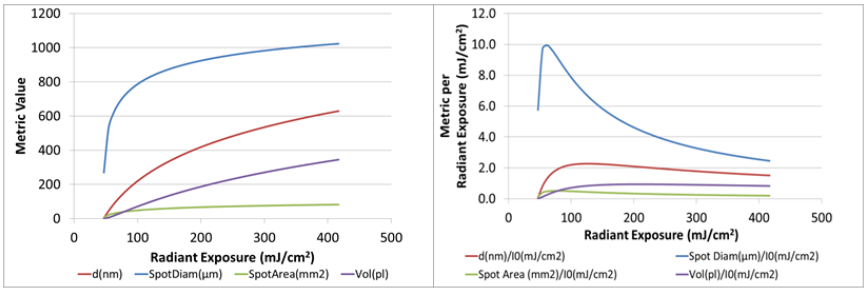

(a) (b)

Fig. 1. **a**. The progression of each metric with the increasing radiant exposure. At threshold fluence, all metrics collapse to zero, they all achieve saturation after the threshold fluence with different rate. The metric spot diameter becomes saturated faster compared to other metrics. The other metrics achieve saturation at higher radiant exposures. **b**. The figure represents how different metrics per radiant exposure behave with respect to the radiant exposure. The optimum for each metric is clearly represented with a peak in the curve. This optimum value is in accordance with Table 1. The metric spot volume has the highest optimum fluence value. Before the optimum fluence, the metric value increases (representing increasing ablation efficiency). Beyond the optimum value the metric value starts to decline (representing reducing ablation efficiency). The rate of increment in efficiency below optimum is observed to be higher compared to the rate of decrement in efficiency beyond optimum.

#192124 - $15.00 USD Received 11 Jun 2013; revised 11 Jul 2013; accepted 11 Jul 2013; published 24 Jul 2013
(C) 2013 OSA

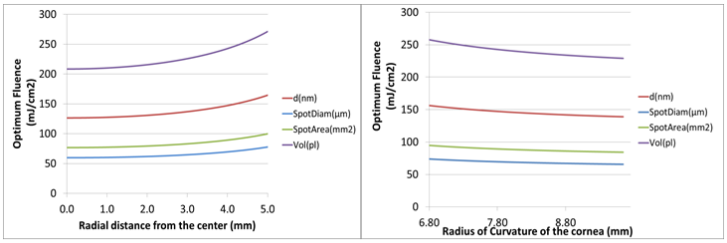

(a) (b)

Fig. 2. **a**. The increase in optimum fluence with the increasing radial distance for a typical radius of curvature (7.81 mm). The increase at the periphery of the cornea can be explained by the changing incidence angle. With the loss of efficiency due to non-normal incidence at the periphery, the optimum fluence value increases for all the metrics. **b**. The progression of optimum fluence for varying radius of curvature at a radial distance of 4 mm from the center of the cornea. For lesser radii of curvature (steeper corneas) the optimum fluence is higher compared to higher radii of curvature (flatter corneas). The optimum value collapses to normal incidence for all the metrics for a flat surface (radius of curvature = ∞).

From the fluctuations observed in energy delivery, the deviations in corneal ablation can be estimated. This effect is shown in Fig. 3.

For a given energy fluctuation, as the radiant exposure increases, the relative ablation deviation decreases. The ablation deviation is the corresponding relative change in the metric value in percentage. This is calculated at random values of radiant exposure. For radiant exposures beyond optimum fluence, ablation deviations are smaller than energy fluctuations. We calculated the ablation deviation for different metrics for a deviation of –20% in the laser beam energy with respect to the radiant exposure. The effects of the energy fluctuation were observed more at lower radiant exposures. As we approached the optimum fluence for the corresponding metric, the effect of energy fluctuations reduced. For instance, at 450 mJ/cm^2, the effects of –20% energy deviation range between –2% (for spot diameter) to –14% (for spot volume).

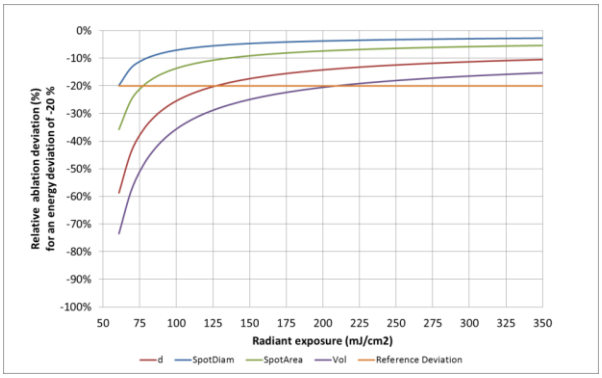

Fig. 3. For a given energy fluctuation (–20% in the figure as reference), as the radiant exposure increases, the relative ablation deviation decreases. For all metrics at optimum fluence (as per Table 1) relative ablation deviation equals relative energy deviation. For radiant exposures beyond optimum fluence, ablation deviations are smaller than energy fluctuations (Relative ablation deviation < –20% which is the reference energy deviation). For radiant exposures lesser than optimum fluence, ablation deviations are larger than energy fluctuations (increasing slope as the radiant exposure is reduced below optimum fluence). The metric spot volume shows the most sensitive behavior for radiant exposures below optimum fluence. For all metrics, the effect of energy deviation in ablation accounts for –100% (no ablation) close to the threshold. This implies that working at a radiant exposure above and beyond the optimum value can reduce the effects of energy fluctuations on the outcomes by reducing the ablation deviations.

#192124 - $15.00 USD Received 11 Jun 2013; revised 11 Jul 2013; accepted 11 Jul 2013; published 24 Jul 2013
(C) 2013 OSA

Discussion

This study provides analytical expressions for calculation of some optimum ablation parameters for maximizing ablation efficiency and for determination of the fluctuations in corneal ablation from the fluctuations observed in energy delivery. The model directly considers laser beam characteristics and ablative spot properties. Separate analysis of the effect of each parameter was performed.

Several metrics relevant to laser refractive surgery have been proposed and optimized (spot depth, spot diameter, spot area, spot volume). In a sense, these are the metrics characterizing the resolution of the system.

At the core of our calculation is the empirical logarithmic relationship between fluence (energy/area) and ablation rate suggested by Seiler and associates [30,31].

The ablation rate depends on the applied radiant exposure and the super-gaussian order of the beam profile, whereas the deviations in corneal ablation further depend on the fluctuations observed in energy delivery.

Interestingly, none of the fluences optimizing the different metrics depend on the spot, beam sizes or the absorption coefficient of the material.

Maintaining peak radiant exposure constant, as the super-gaussian order of the beam increases, so does the energy per pulse. (Eq. (5) allows computing I_0 as a function of N for a constant pulse E).

Radiant exposure plays the most important role in the determination of ablation rates. The range for radiant exposures of the excimer laser systems for refractive surgery available in the market runs from about 90 mJ/cm^2 to about 500 mJ/cm^2. Super-gaussian order of the beam energy profile runs from 1 (simple gaussian profile) to ∞ (representing a flat-top beam profile). Since the super-gaussian order of the beam is not always known, the values for simple gaussian and flat-top profiles can be considered as the upper and lower bounds of the optimization.

Modifying the super Gaussian profile by increasing the exponent N to infinite results in a "top hat" profile with the same constant radiant exposure over the entire spot diameter. Consequently, one has to increase the single pulse energy to achieve such a change in the beam profile and, as a result, one can observe a higher ablation volume for each single pulse. From our analysis, we observe that for the metrics for which the super Gaussian order of the beam is relevant, for a higher value of N the optimum fluence gets lower.

From the fluctuations observed in energy delivery, the deviations in corneal ablation can be estimated. For a given energy fluctuation, as the radiant exposure increases, the relative ablation deviation decreases. Beyond the optimum fluence, the effect of energy fluctuations on ablation deviations is lesser compared to radiant exposures below optimum.

There is another way of interpreting optimum efficiency in terms of rate of change as shown in Fig. 3 for the metric spot volume. The rate of change of the selected metric with respect to the radiant exposure can be compared with metric value per radiant exposure. At the optimum fluence for a given metric, the rate of change vs. radiant exposure equals unity (so relative energy fluctuations correspond 1:1 to relative ablation deviations). This can be explained with the effect of energy fluctuations on different metrics with respect to the radiant exposure (Fig. 3). Below optimum, relative energy fluctuations are "amplified" in larger relative ablation deviations (i. e. investing a bit more energy, drastically increases ablation rate). Beyond optimum, relative energy fluctuations are "attenuated" in smaller relative ablation deviations (i. e. to slightly increase ablation rate, much more energy shall be invested). Additionally, the rate of increment in efficiency below optimum is observed to be higher compared to the rate of decrement in efficiency beyond optimum. (Fig. 1(a) and 1(b)). In Fig. 3, for explanatory purposes, the energy fluctuation was set at −20% level, this does not correspond to a realistic value, but it helps to understand the key concept of amplifying versus attenuating the energy fluctuation.

#192124 - $15.00 USD Received 11 Jun 2013; revised 11 Jul 2013; accepted 11 Jul 2013; published 24 Jul 2013
(C) 2013 OSA

We have shown that the relative energy fluctuations do not correspond one-to-one with the impact in deviations in corneal ablation. For a gaussian beam of 160 mJ/cm^2 nominal radiant exposure, a severe energy overshoot of + 50% corresponds to an "amplified" overcorrection of + 75% on corneal tissue, whereas for 500 mJ/cm^2 nominal radiant exposure, it corresponds to an "attenuated" overcorrection of + 35% on corneal tissue. As well, the values for simple Gaussian and flat-top profiles can be considered as the lower and upper bounds of the corneal relative deviation.

For the selected valuable metric to be optimized (typically spot volume) the final determined value shall be equal or higher than the theoretical optimum (in order to get the very high ablation efficiency for this energy, but attenuated relative deviations). Similarly, if one considers the effect of non-normal incidence, we advocate using the maximum value of the chosen metric, such that it covers the effect of non-normal incidence at sufficient radial distances from the center as well as sufficient radius of curvature for different patients.

The calculation of the final optimum fluence depends mainly on two factors. First, the total number and kind of metrics being considered for optimization of the ablation efficiency and second the energy fluctuations of the system. Therefore, the final radiant exposure can be calculated in two steps in order to account for the aforementioned factors. In the first step the optimum fluence for the considered metric is calculated. In case one considers multiple metrics the optimum fluence highest amongst the considered metrics should be chosen. This fluence value covers the other considered metrics indirectly. In the second step the calculated optimum fluence can be added with a factor that accounts for the fluctuations in energy (as calculated with Eq. (8)). Adding this factor shall provide additional stability from the energy fluctuations of the system. For excimer laser systems, energy deviation typically lies between ± 3% to ± 5% Root-Mean-Square (RMS). Considering the RMS as one standard deviation, we arrive at ± 8% energy deviation for a typical excimer laser system. Hence, we propose to add + 8% to the analytically calculated optimum fluence. This factor will ensure that the fluence level will remain above the optimum even if energy instability is introduced because of the system itself.

We consider spot volume as most valuable metric for two reasons, one to reduce the amount of energy delivered for the total ablation volume and second since it requires the highest optimum (Fig. 1(b)) so all other metrics even without being considered directly, are already in the stable regions. The ablation resolution is also made more stable for the optimum criteria as the beam size saturates quickly after optimum. Furthermore, the radiant exposure optimized for the spot volume shall reduce the thermal effects induced in the tissue. The thermal load from a laser pulse is directly proportional to the radiant exposure (Eq. (17)) and hence to the pulse energy (Eq. (5)). Minimizing the amount of energy delivered for the total ablation volume means minimizing the total thermal load.

$$\Delta T = \frac{\alpha}{\rho \cdot c} I_0 . (1 - \mathrm{R}) \tag{17}$$

where, ΔT represents thermal load occurring at the end of the laser pulse, α is the absorption coefficient of the tissue, ρ is the density of the tissue, c is the specific heat and R is the reflectivity of the tissue, I_0 represents the radiant exposure on the tissue.

For example, from Fig. 2(a) and 2(b) we can choose an optimum fluence of ~250 mJ/cm^2. This value shall cover all the presented metrics as well as the effect of non-normal incidence up to the radial distance of 4 mm (from the center of the cornea) and a range of patients with radius of curvature of 7.2 mm and beyond.

This model can be easily generalized to any material for which the absorption coefficient and the ablation threshold for the specific wavelength and laser characteristics are known.

The model described here provides analytical expressions for optimizing several valuable metric, based upon comprehensive parameters. The proposed model provides results

#192124 - $15.00 USD Received 11 Jun 2013; revised 11 Jul 2013; accepted 11 Jul 2013; published 24 Jul 2013
(C) 2013 OSA

consistent to those observed in the literature [32]. Additionally, it offers an analytical expression including some parameters that were ignored (or at least not directly addressed) in previous analytical approaches. This model may complement previous analytical approaches to the efficiency problem and may sustain the observations reported by others.

Adding another dimension to the results presented here is the criteria, repetition rate. The repetition rate of the laser can also be optimized for all the metrics mentioned above. The radiant exposure is linearly related to the single pulse energy. (From Eq. (5)). The pulse energy is a function of the average power and the repetition rate of the laser. Typically with an increase in the repetition rate, a decrease in single pulse energy is observed. If an exact relation between the single pulse energy and repetition rate is known, all the metrics can be optimized for repetition rate with a similar method [33].

Even though a large number of detailed parameters are considered, this model is still characterized by a relatively low degree of complexity.

Huang et al. [34], investigated the effect of laser spot size on the outcome of aberration correction with scanning laser corneal ablation using numerical simulation of ablation outcome of correction of wavefront aberrations of Zernike modes from second to eighth order. They modeled Gaussian and top-hat beams from 0.6 to 2.0-mm full-width-half-maximum diameters and evaluated the fractional correction and secondary aberration (distortion), and used a distortion/correction ratio of less than 0.5 as a cutoff for adequate performance. They found that a 2 mm or smaller beam is adequate for spherocylindrical correction (Zernike second order), a 1 mm or smaller beam is adequate for correction of up to fourth order Zernike modes, and a 0.6 mm or smaller beam is adequate for correction of up to sixth order Zernike modes.

Guirao et al. [35], calculated that the success of a customized laser surgery attempting to correct higher order aberrations depends on using a laser beam that is small enough to produce fine ablation profiles needed to correct higher order aberrations. Simulating more than 100 theoretical customized ablations performed with beams of 0.5, 1.0, 1.5, and 2.0 mm in diameter, they calculated the residual aberrations remaining in the eye and estimated the modulation transfer function (MTF) from the residual aberrations. They found that the laser beam acts like a spatial filter, smoothing the finest features in the ablation profile and that the quality of the correction declines steadily when the beam size increases. A beam of 2 mm was capable of correcting defocus and astigmatism. Beam diameters of 1 mm or less may effectively correct aberrations up to fifth order.

Petit [36], claimed that the LADARVision system using a small fixed diameter excimer laser beam providing a consistent ablation per pulse, is able to ablate complex (higher order) corneal shapes accurately. He also explored the optimum ablation depth per laser pulse to optimize the ablation efficiency [32]. Our work takes this idea forward by including other important criteria for optimization. These additions specify the optimized laser characteristics in a more holistic manner.

As demonstrated by Pedder et al. [37], and Jiménez et al. [38], the incorporation of models taking into account the angular dependence of laser-ablation rates as well as the effect of plume absorption, can be important in efforts to improve the ablation algorithms used in refractive surgery. The high accuracy of determination of stroma plume absorption coefficients and the incorporation of this information in laser-ablation equations can improve the prediction of postsurgical corneal shape. More accurate values for postsurgical radius and asphericity could be achieved and thereby enhance emmetropization and correction of eye aberrations in refractive surgery. However, in some systems, the effect of the ablation plume could be not so significant since a debris removal system is incorporated [39].

Clinical evaluations on human eyes are needed to confirm the preliminary simulated results presented herein. Accurate knowledge for the absorption coefficient of the human cornea is imperative in validating the presented results.

#192124 - $15.00 USD Received 11 Jun 2013; revised 11 Jul 2013; accepted 11 Jul 2013; published 24 Jul 2013
(C) 2013 OSA

Conclusions

The model introduced in this study provides an analytical expression for optimizing ablation parameters. The model incorporates several factors that were ignored in previous analytical models. Furthermore, due to its analytical approach, it is valid for different laser devices used in refractive surgery, as well as for any materials for which the coefficients and the ablation characteristics for the specific laser system are known.

The development of more accurate models to improve emmetropization and the correction of ocular aberrations is an important issue. We hope that this model will be an interesting and useful contribution to refractive surgery and will take us one-step closer to this goal.

Acknowledgments

The article has not been presented at any meeting. The authors did not receive any financial support from any public or private sources. The authors have no financial or proprietary interest in a product, method, or material described herein. But they are both employees of SCHWIND eye-tech-solutions. The article represents the personal views of the Authors, and was not written as a work for hire within the terms of the Author's employment with SCHWIND eye-tech-solutions. The work described in the article itself (as opposed to the work done writing the article) was conducted as part of the Author's work for SCHWIND eye-tech-solutions. Content attributed to the Authors was vetted by a standard SCHWIND eye-tech-solutions approval process for third-party publications.

#192124 - $15.00 USD Received 11 Jun 2013; revised 11 Jul 2013; accepted 11 Jul 2013; published 24 Jul 2013
(C) 2013 OSA